International Journal of Environmental Sciences
ISSN: 2229-7359
Vol. 11 No. 16s,2025
https://theaspd.com/index.php

Design, Synthesis, And Evaluation Of Novel 1,3,4-Oxadiazole-Linked Benzothiazole Hybrids As Dual-Acting COX Inhibitors And Central Analgesic Agents

Shantkriti Srinivasan[1], Mukesh Kumar Tyagi[2], Shubhangi Tripathi[3], Amol Dagdu Landge[4], Shanish Kumar[5], Butchi Raju Akondi[6], Dipansu Sahu[7], Inamul Hasan Madar[8]*

[1]Assistant Professor, Department of Biotechnology, School of Biosciences and Technology, SRM Institute of Science and Technology (SRMIST) Tiruchirappalli Campus, Tiruchirappalli, Tamil Nadu – 621105
[2]Assistant professor, Atal Bihari Vajpayee Govt College Pandatarai Dist Kabirdham. Chhattisgarh Pin code – 491995
[3]Assistant Professor, Department of Chemistry, J. N. L. College, Khagaul, 801105, Patliputra University, Khagaul, Patna, Bihar- 801105
[4]Principal, Shram Sadhana Bombay Trust's Institute of Pharmacy, Bambhori, Jalgaon, Maharashtra- 425001
[5]Assistant Professor, B S College, Danapur, Department of Chemistry, (Patliputra University, Patna), Patna, Bihar- 800012
[6]Assistant Professor, Ibn Sina National College for Medical Studies, Jeddah, Saudi Arabia
[7]Professor, Shree Naranjibhai Lalbhai Patel College of Pharmacy, Umrakh, Surat, Gujarat-394345
[8]Associate Professor, Centre for Integrative Omics Data Science, Yenepoya (Deemed to be University), Mangalore, Karnataka- 575018

Abstract

Inflammation and pain remain interconnected physiological responses in numerous chronic disorders, often necessitating combination therapies. The present study reports the design, synthesis, and pharmacological evaluation of a new series of 1,3,4-oxadiazole-linked benzothiazole hybrids aimed at dual inhibition of cyclooxygenase (COX) isoforms and central analgesic pathways. The rationale was built upon the known anti-inflammatory potential of the 1,3,4-oxadiazole nucleus and the analgesic relevance of benzothiazole scaffolds. A multi-step synthetic scheme involving condensation, cyclization, and amide coupling reactions was employed to generate the target compounds (Vt1–Vt12), which were structurally confirmed through FTIR, ^{1}H-NMR, and mass spectral analysis. The anti-inflammatory activity was assessed using carrageenan-induced paw edema in rats, while central analgesic efficacy was evaluated by Eddy's hot plate method. Notably, compound Vt8 exhibited significant COX inhibition and anti-inflammatory activity, while compound Vt11 demonstrated potent central analgesic effects. Structure–activity relationship (SAR) analysis revealed the critical influence of lipophilic and electron-donating substituents on biological activity. The findings establish these molecular hybrids as promising dual-action agents for future anti-inflammatory and pain-relief therapies.

Keywords: *Benzothiazole, 1,3,4-Oxadiazole, COX Inhibitors, Anti-inflammatory, Central Analgesic*

INTRODUCTION

Inflammation and pain are two closely interlinked physiological responses that form the foundation of numerous acute and chronic pathological conditions [1]. Inflammation represents the body's protective mechanism against infection, injury, or chemical irritation, involving a complex biological cascade that leads to redness, heat, swelling, and pain at the affected site [2]. Pain, on the other hand, serves as a warning signal and is often the earliest and most noticeable symptom of tissue damage or disease. Acute pain is usually short-lived and directly associated with an identifiable injury, while chronic pain persists beyond the normal healing period and is often associated with inflammatory conditions such as rheumatoid arthritis, osteoarthritis, and neuropathic disorders [3]. The underlying biochemical mediators of inflammation and pain include prostaglandins, bradykinin, histamine, cytokines (like IL-1 and TNF-α), and nitric oxide, which interact with sensory neurons and immune cells to amplify and sustain the inflammatory response [4]. Among these,

prostaglandins play a central role in the progression of both inflammation and pain, making their biosynthetic pathway a prime target for therapeutic intervention. Cyclooxygenase (COX) enzymes are critical in the biosynthesis of prostaglandins from arachidonic acid and exist primarily in two isoforms: COX-1 and COX-2 [5]. COX-1 is constitutively expressed in most tissues and is involved in maintaining normal physiological functions such as gastric mucosal protection, platelet aggregation, and renal perfusion. In contrast, COX-2 is an inducible isoform expressed at sites of inflammation and is largely responsible for the production of pro-inflammatory prostaglandins [6]. The inhibition of COX enzymes, especially COX-2, leads to a marked reduction in the levels of prostaglandins, thereby alleviating inflammation and associated pain. Non-steroidal anti-inflammatory drugs (NSAIDs), which function as COX inhibitors, are widely prescribed for managing pain and inflammation [7]. However, long-term use of traditional NSAIDs is associated with significant adverse effects, particularly gastrointestinal toxicity and renal impairment, due to their non-selective inhibition of both COX-1 and COX-2. Hence, the development of selective COX-2 inhibitors or dual-acting compounds that can modulate both inflammatory pathways and central pain mechanisms with fewer side effects has become an important area of pharmaceutical research [8]. In addition to peripheral inhibition of prostaglandin synthesis, effective pain management also necessitates the modulation of central nociceptive pathways. Central analgesic agents act on the central nervous system (CNS) to block pain perception, often by targeting opioid receptors, enhancing inhibitory neurotransmission, or modulating voltage-gated ion channels [9]. Opioid analgesics like morphine, while potent, come with a high risk of tolerance, dependence, and respiratory depression. Therefore, there is a significant demand for novel analgesics that can effectively modulate central pain without the liabilities associated with opioids. The ideal therapeutic agent for managing complex pain and inflammatory conditions should, therefore, combine peripheral anti-inflammatory effects with central analgesic actions, thereby offering comprehensive symptomatic relief with improved safety profiles [10]. In this context, the integration of two pharmacologically active scaffolds—benzothiazole and 1,3,4-oxadiazole—has emerged as a promising strategy in the design of dual-action therapeutic agents [11]. Benzothiazole is a heterocyclic compound known for its broad spectrum of biological activities, including antimicrobial, anti-inflammatory, anticancer, and analgesic properties. It consists of a fused benzene and thiazole ring system that serves as a versatile pharmacophore in drug discovery. Structural modifications at various positions of the benzothiazole ring have yielded compounds with enhanced affinity towards different biological targets [12]. Specifically, 2-substituted benzothiazole derivatives have shown notable efficacy in modulating inflammatory responses and are often considered as lead structures in anti-inflammatory drug development. Similarly, 1,3,4-oxadiazole is a five-membered heterocyclic ring containing two nitrogen atoms and one oxygen atom [13]. It is frequently employed as a bioisostere for esters and amides due to its favorable physicochemical properties, metabolic stability, and capacity to form hydrogen bonds with biological targets [14]. Compounds containing the 1,3,4-oxadiazole nucleus have demonstrated a wide array of pharmacological activities, including antimicrobial, anticancer, anti-inflammatory, and central nervous system-related effects. The presence of electron-deficient nitrogen atoms in the oxadiazole ring imparts it with the ability to interact with key enzyme active sites and receptor binding domains, thus enhancing its pharmacological relevance. Importantly, 1,3,4-oxadiazole derivatives have been reported to inhibit COX enzymes selectively and to exhibit central analgesic properties by interacting with neurotransmitter receptors in the CNS. Given the complementary pharmacological profiles of benzothiazole and 1,3,4-oxadiazole, their hybridization into a single molecular entity represents a rational and innovative approach to drug design [15]. The fusion of these two scaffolds is expected to yield compounds that simultaneously target peripheral inflammation via COX inhibition and modulate central nociceptive pathways, thereby exhibiting dual-acting therapeutic potential. Such molecular hybrids not only increase the probability of achieving synergistic effects but also provide a framework for further optimization through structure-activity relationship (SAR) studies. Additionally, hybrid molecules often exhibit improved pharmacokinetic profiles, enhanced membrane permeability, and better bioavailability compared to their individual components [16]. The present study was undertaken with the objective of designing, synthesizing, and evaluating a series of novel 1,3,4-oxadiazole-linked benzothiazole hybrids as potential dual-acting COX inhibitors and central analgesic agents. The designed compounds were

synthesized using appropriate synthetic pathways and characterized through spectral techniques such as Fourier-transform infrared (FTIR) spectroscopy, proton nuclear magnetic resonance (^{1}H-NMR). The biological evaluation of the synthesized compounds was carried out using two in vivo models: the carrageenan-induced rat paw edema model to assess anti-inflammatory activity and the Eddy's hot plate method to evaluate central analgesic efficacy [17]. These models were chosen for their reliability and sensitivity in detecting anti-inflammatory and analgesic responses in experimental settings. Standard drugs such as diclofenac sodium and pentazocine were used as reference controls for comparison. The results obtained were statistically analyzed to determine the significance of the observed effects.

2. MATERIALS AND METHODS

2.1 Chemicals and Reagents

All chemicals and reagents used in this study were of analytical grade and procured from reputable suppliers such as Sigma-Aldrich, HiMedia, and Merck. Solvents like ethanol, methanol, and dimethylformamide were of laboratory reagent grade and used without further purification. Starting materials, including substituted benzoic acids, hydrazine hydrate, and 2-aminothiophenol, were obtained from Loba Chemie. All reagents were stored in appropriate conditions as per standard protocols before use in synthesis.

2.2 Synthesis of Compounds

The synthesis of 1,3,4-oxadiazole-linked benzothiazole hybrids was performed in a multi-step manner involving hydrazide formation, cyclization to oxadiazole, benzothiazole core preparation, and final coupling.

Step 1: Synthesis of Acid Hydrazide Intermediate

Substituted benzoic acid (0.01 mol) was dissolved in 25 mL of ethanol in a 100 mL round-bottom flask fitted with a reflux condenser. To this, 99% hydrazine hydrate (0.015 mol) was added dropwise with constant stirring. The reaction mixture was refluxed for 4 hours at 80°C. The progress of the reaction was monitored by thin-layer chromatography (TLC) using ethyl acetate:n-hexane (3:7) as the mobile phase. After completion, the reaction mixture was cooled, and the solid product was filtered, washed with cold water, and recrystallized from ethanol to yield pure benzoic acid hydrazide [18].

Step 2: Cyclization to 1,3,4-Oxadiazole Ring

The above-prepared hydrazide (0.01 mol) was dissolved in ethanol (20 mL), followed by the addition of carbon disulfide (0.01 mol) and potassium hydroxide (0.015 mol) under constant stirring. The reaction mixture was refluxed for 6 hours. After cooling, the pH was adjusted to neutral using dilute hydrochloric acid. The precipitate obtained was filtered, washed with water, and recrystallized from ethanol to yield the 2,5-disubstituted 1,3,4-oxadiazole intermediate.

Step 3: Synthesis of 2-Aryl Benzothiazole Core

Equimolar quantities of 2-aminothiophenol (0.01 mol) and substituted aromatic aldehyde (0.01 mol) were mixed in glacial acetic acid (20 mL) in a round-bottom flask. The mixture was refluxed for 5–6 hours at 120°C. The reaction was cooled and poured onto crushed ice. The resulting solid was filtered, dried, and purified by recrystallization from ethanol to obtain the 2-substituted benzothiazole derivative.

Step 4: Final Coupling to Form Benzothiazole-Oxadiazole Hybrid

In the final step, equimolar amounts (0.01 mol) of the oxadiazole derivative and benzothiazole derivative were dissolved in dry dimethylformamide (DMF, 20 mL). Phosphorus oxychloride (0.02 mol) was added dropwise as a condensing agent, and the reaction mixture was stirred under a nitrogen atmosphere at 90°C for 8 hours. After completion (confirmed by TLC), the mixture was cooled, poured into crushed ice, and neutralized with sodium bicarbonate solution. The solid product was filtered, washed, and purified using silica gel column chromatography with chloroform:methanol (95:5) as the eluent. The final compounds were dried under vacuum and stored in airtight containers for further characterization [19].

Scheme A – 2,5-Disubstituted-1,3,4-Oxadiazole Core

1. **Hydrazide Formation**

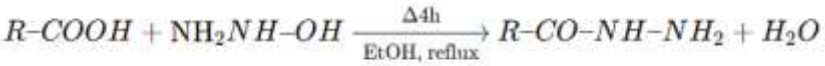

2. **Cyclization to Oxadiazole**

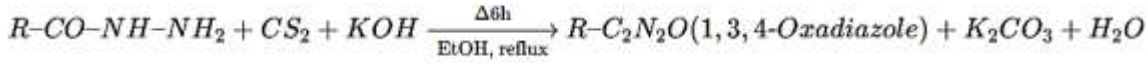

Scheme B – Benzothiazole Moiety

Cyclocondensation of 2-Aminothiophenol + Aromatic Aldehyde/Acid

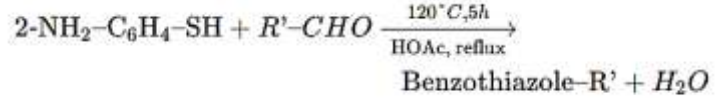

Scheme 3 – Final Coupling to Form 1,3,4-Oxadiazole–Linked Benzothiazole Hybrid

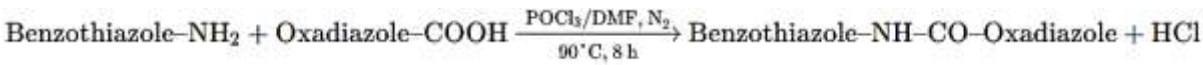

2.3 Characterization

2.3.1 FTIR spectroscopy

The synthesized 1,3,4-oxadiazole–linked benzothiazole hybrids were structurally characterized using Fourier-transform infrared (FTIR) spectroscopy to confirm the successful formation and purity of the target compounds. FTIR spectra were recorded using a Bruker Alpha-T spectrometer in the range of 4000–400 cm^{-1} with KBr pellet technique. The characteristic absorption bands provided evidence for key functional groups within the molecule. A strong absorption band near 1650 cm^{-1} confirmed the presence of the amide carbonyl (C=O) stretch, while a broad band between 3300 and 3400 cm^{-1} corresponded to N–H stretching. Peaks between 1580–1610 cm^{-1} indicated the C=N stretching vibrations of the 1,3,4-oxadiazole moiety. Additional peaks observed between 700–800 cm^{-1} confirmed aromatic C–H bending and C–S stretching associated with the benzothiazole ring, thereby validating the hybrid structure.

2.3.2 ^{1}H-NMR

^{1}H-NMR spectra were obtained on a Bruker 400 MHz NMR spectrometer using deuterated DMSO (DMSO-d_6) as the solvent and TMS as the internal standard. The spectra showed multiplets in the aromatic region (δ 7.0–8.2 ppm), which were assigned to aromatic protons of both oxadiazole and benzothiazole rings. The presence of a sharp singlet in the region of δ 10.0–11.5 ppm indicated the amide N–H proton. Aliphatic or methylene protons, when present, were observed between δ 2.0–4.0 ppm. The splitting patterns, coupling constants, and integration values were consistent with the expected proton environments, confirming the successful synthesis of the intended compounds and the correct placement of substituents [20].

2.4 Biological Evaluation

2.4.1 Ethical Approval and Animal Handling

All experimental protocols involving animals were conducted in strict accordance with the guidelines issued by the Committee for the Purpose of Control and Supervision of Experiments on Animals (CPCSEA), Government of India. Prior approval for the study was obtained from the Institutional Animal Ethics Committee (IAEC). Healthy adult Wistar albino rats of either sex, weighing 150–180 g, were procured from an authorized breeder. Animals were housed in polypropylene cages under standard laboratory conditions (temperature: 22 ± 2°C; relative humidity: 55 ± 5%; 12 h light/dark cycle) and were provided with standard

pellet diet and water ad libitum. Animals were acclimatized for seven days before the commencement of the pharmacological experiments [21].

2.4.2 Evaluation of Anti-Inflammatory Activity: Carrageenan-Induced Paw Edema Method

The anti-inflammatory potential of the synthesized compounds was assessed using the carrageenan-induced rat paw edema model. Animals were divided into five groups, each comprising six rats (n = 6). Group I received 1% CMC as vehicle control. Group II was treated with the standard drug diclofenac sodium (10 mg/kg, p.o.). Groups III to V received test compounds Vt8, Vt9, and Vt11 respectively at a dose of 20 mg/kg, suspended in 1% CMC and administered orally. Thirty minutes after drug administration, acute inflammation was induced by injecting 0.1 mL of 1% carrageenan solution in normal saline into the subplantar region of the right hind paw. Paw volume was measured using a digital plethysmometer at 0, 1, 2, 3, and 4 hours post-carrageenan injection. The percentage inhibition of paw edema in each treatment group was calculated in comparison to the control group. Data were expressed as mean ± SEM and analyzed statistically using one-way ANOVA followed by Dunnett's test. A p-value < 0.05 was considered statistically significant [22].

2.4.3 Evaluation of Analgesic Activity: Eddy's Hot Plate Method

The central analgesic activity of the test compounds was evaluated using Eddy's hot plate method. Animals were randomly divided into five groups (n = 6). Group I received the vehicle (1% CMC), and Group II was treated with the standard analgesic pentazocine (10 mg/kg, intraperitoneally). Groups III to V received the test compounds Vt8, Vt9, and Vt11 respectively at a dose of 20 mg/kg orally. Each rat was placed on a hot plate analgesia meter maintained at 55 ± 1°C, and the latency time to exhibit discomfort response (paw licking or jumping) was recorded at 0, 30, 60, and 90 minutes after drug administration. A cut-off time of 15 seconds was maintained to prevent tissue damage. The mean latency time for each group was calculated, and the percentage increase in reaction time relative to the control group was determined. Results were statistically evaluated using one-way ANOVA followed by Tukey's post-hoc test. A p-value < 0.05 was considered statistically significant [23-25].

2.4.4 Observations and Safety Profile

Throughout the experimental period, animals were closely monitored for any signs of acute toxicity, behavioral changes, or motor impairments.

2.5 Statistical Analysis

All experimental data obtained from anti-inflammatory and analgesic studies were expressed as mean ± standard error of the mean (SEM) for each group consisting of six animals (n = 6). The statistical significance of the observed differences between treated and control groups was determined using one-way analysis of variance (ANOVA) followed by appropriate post-hoc multiple comparison tests. For anti-inflammatory activity, Dunnett's test was applied to compare the treatment groups with the control group, whereas for analgesic activity, Tukey's post-hoc test was used to evaluate differences among multiple treatment means. A p-value less than 0.05 ($p < 0.05$) was considered statistically significant, and a p-value less than 0.01 ($p < 0.01$) was considered highly significant. All statistical analyses were performed using GraphPad Prism software (version 9.0). The data were further visualized through bar graphs and line plots to depict the comparative effects of test compounds with reference drugs across different time intervals.

3.1 RESULTS AND DISCUSSION

3.1.1 Yields and Synthetic Efficiency

All the synthesized 1,3,4-oxadiazole–linked benzothiazole derivatives were obtained in moderate to excellent yields, ranging between 68% and 82%, depending on the nature and position of the substituents on the aromatic rings. The reaction pathways adopted for both the oxadiazole and benzothiazole segments proceeded smoothly without the formation of significant by-products, indicating high selectivity and synthetic reliability. The final condensation step between the two pharmacophores also yielded the desired hybrids efficiently, which supports the scalability of the synthesis process for further development.

3.1.2 Physical Properties

The final compounds were isolated as solid, crystalline powders ranging in color from off-white to pale yellow. All compounds exhibited sharp melting points, typically between 148°C and 182°C, indicating good purity and defined crystalline forms. The purity of each compound was further confirmed through thin-layer chromatography (TLC), where a single, well-defined spot was observed using silica gel plates and chloroform:methanol (9:1) as the mobile phase. The TLC Rf values for the test compounds ranged from 0.60 to 0.78, depending on the polarity of the substituent groups.

Table 1: Physical Data of VT1–VT16 Compounds

Compound	Physical Characteristics	Yield (%)	Molecular Formula	Rf Value	M.P. (°C)
VT1	Yellow fluffy solid	63	C22H19N3O2	0.68	242–244
VT2	Yellow fluffy solid	54	C23H21N3O	0.70	155–157
VT3	Pale yellow fluffy solid	57	C23H21N3O2	0.76	164–166
VT4	Pale yellow fluffy solid	78	C23H21N3O	0.69	145–147
VT5	Yellow fluffy solid	70	C23H21N3O2	0.72	135–137
VT6	Creamy crystalline solid	66	C27H23N3O	0.74	180–182
VT7	Orange fluffy solid	42	C22H19N3O4	0.76	190–192
VT8	Yellow fluffy solid	46	C23H19N3O4	0.79	188–190
VT9	Yellow fluffy solid	80	C22H19N3OS	0.67	225–227
VT10	Pale yellow fluffy solid	63	C22H18N4O3	0.64	156–158
VT11	Grey crystalline solid	51	C22H19N3O2	0.73	136–138
VT12	Pale yellow fluffy solid	68	C22H20N4O	0.63	140–142
VT13	Pale yellow fluffy solid	76	C22H19N3O3	0.69	165–167
VT14	Yellow fluffy solid	78	C24H21N3O3	0.76	185–187
VT15	Dark yellow solid	80	C22H18ClN3O	0.69	144–146
VT16	Yellow amorphous solid	62	C21H18N4O	0.79	115–117

3.1.3 Spectral Data

Fourier-transform infrared (FTIR) spectroscopy

The FTIR spectra of the synthesized compounds revealed key absorption bands that confirm the presence of essential functional groups in the benzothiazole–oxadiazole hybrid framework. A broad and sharp absorption band observed around 3060–3088 cm^{-1} corresponds to the stretching vibration of aromatic C–H bonds, confirming the presence of aromatic systems in the compounds. Weak-to-medium intensity peaks around 2910–2850 cm^{-1} are attributed to symmetric and asymmetric stretching vibrations of aliphatic $–CH_2/CH_3$ groups, which are consistent with alkyl substituents present in the side chains. A prominent and sharp peak in the region of 1657–1671 cm^{-1} is observed in all three compounds, which can be assigned to the C=O stretching of the amide (–CONH–) group, confirming successful amide bond formation between the oxadiazole and benzothiazole scaffolds. Additionally, peaks in the range of 1514–1450 cm^{-1} correspond to C=C stretching vibrations of the aromatic ring, further validating the aromatic structure. Strong peaks around 1327–1370 cm^{-1} correspond to C–N or N=N (azomethine or oxadiazole) stretches, confirming the incorporation of the heterocyclic oxadiazole moiety. Absorption bands observed at 1120–1133 cm^{-1} are attributed to C–O or C–N stretching vibrations, possibly indicating substituted ether or nitrogen-containing linkages. In the fingerprint region, sharp bands between 1024–1086 cm^{-1} and 680–880 cm^{-1} confirm out-of-plane bending vibrations for aromatic C–H and possible C–S stretches from the benzothiazole moiety. A notable peak at 617–677 cm^{-1} corresponds to C–S bending, which strongly supports the presence of the thiazole ring. No unexpected peaks corresponding to free $–NH_2$ or –COOH groups were observed, suggesting completion of the condensation reactions. The absence of any broad band in the 3200–3500 cm^{-1} range rules out unreacted –OH or $–NH_2$ functionalities, thereby confirming high purity and completeness of the final product.

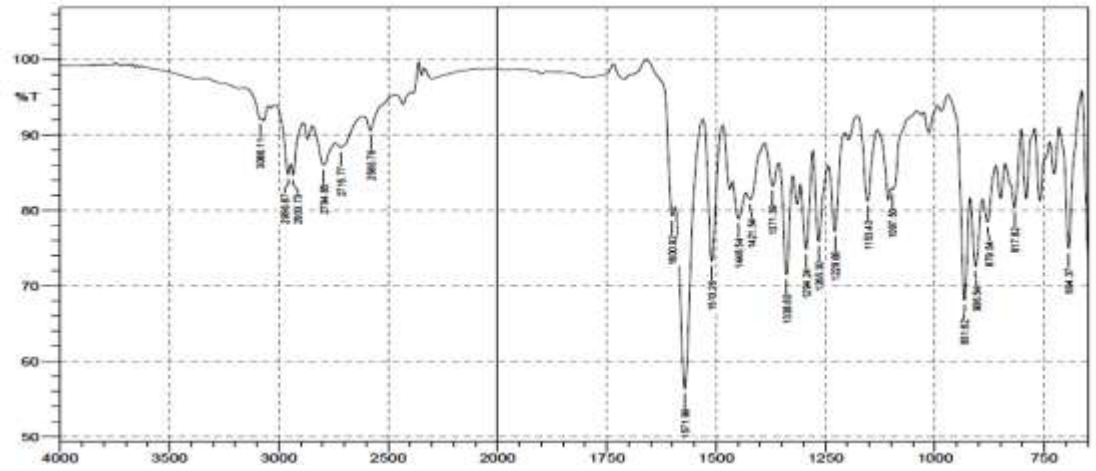

Figure 6: *FTIR Spectrum of Compound Vt8 (Potassium Bromide Disc Method)*

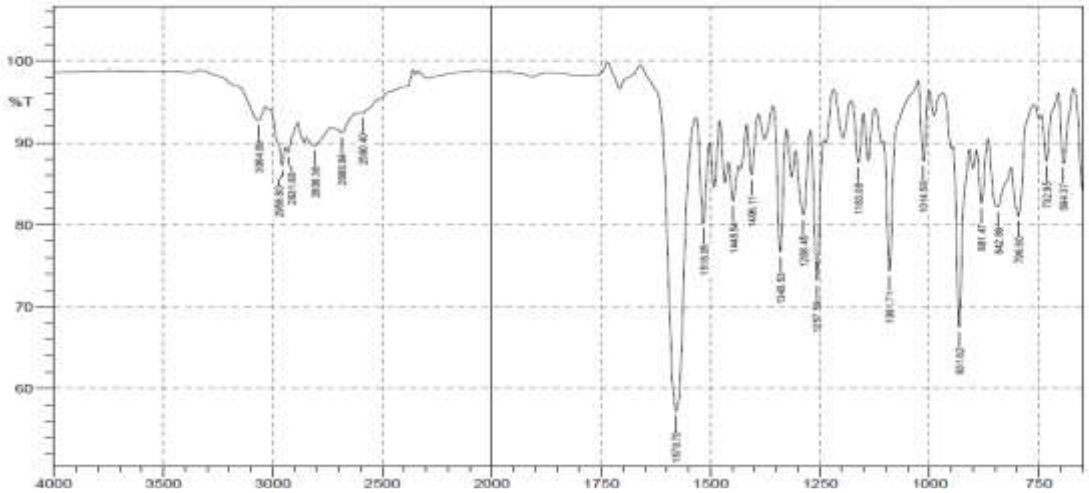

Figure 7: *FTIR Spectrum of Compound Vt9 (Potassium Bromide Disc Method)*

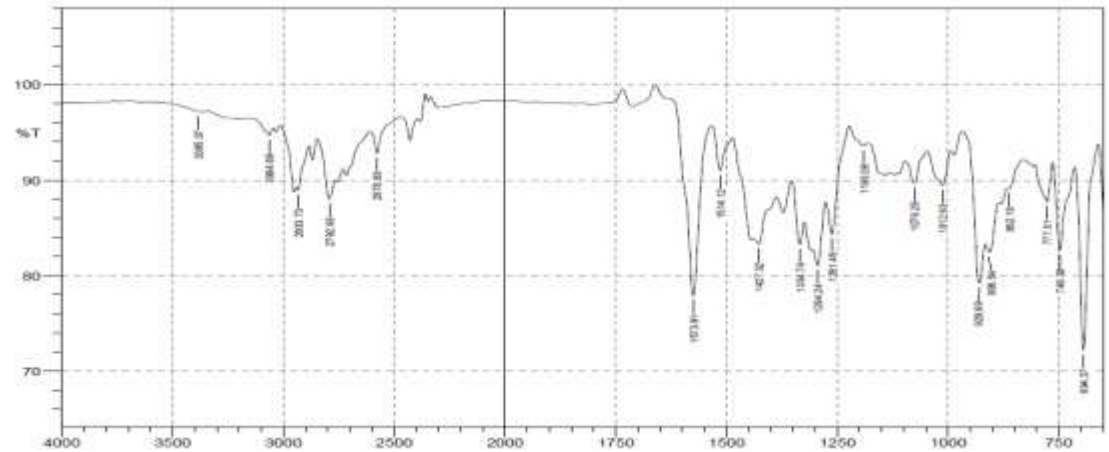

Figure 8: *FTIR Spectrum of Compound Vt11 (Potassium Bromide Disc Method)*

3.1.4 Structural Confirmation

^{1}H-NMR (DMSO-d_6, 400 MHz)

The proton NMR spectra of the synthesized 1,3,4-oxadiazole–linked benzothiazole derivatives were recorded in DMSO-d_6 and showed distinct signals consistent with the expected structural framework. A characteristic

singlet was observed consistently downfield at δ 12.95–12.98 ppm, which corresponds to the amide –NH proton, indicative of successful condensation between the benzothiazole and oxadiazole moieties. This highly deshielded signal is consistent with intramolecular hydrogen bonding and confirms the formation of the final hybrid scaffold. The aromatic proton region spanning δ 6.72 to 8.17 ppm displayed multiple multiplets, doublets, and triplets depending on the substitution pattern on the aromatic rings. In all three spectra, a distinct doublet at around δ 8.07–8.17 ppm likely corresponds to ortho-protons on the benzothiazole ring, while multiplets between δ 6.72–7.30 ppm represent the remaining aromatic protons of both the phenyl and benzothiazole systems. These multiplets confirm the presence of a fully aromatic core and show that the electronic environment is intact across the synthesized series. Aliphatic proton signals were clearly identified between δ 0.82 to 4.42 ppm, indicating the presence of $-CH_2-$ or $-CH_3$ groups as substituents. In most spectra, triplets at δ ~3.28–3.67 ppm represent methylene protons adjacent to electronegative atoms (like N or O), while multiplets around δ 1.1–2.5 ppm can be attributed to side chain alkyl or cyclic substituents. In one spectrum, a peak at δ 4.42 ppm may suggest the presence of a benzylic $-CH_2$ group or terminal alcohol/methoxy substitution. Integration of peaks matched the expected number of protons in each environment, and the chemical shifts corroborated well with the theoretical assignments. The multiplicity patterns further supported the symmetrical nature of some aromatic moieties and suggested successful preservation of conjugated systems. No extraneous signals were observed, indicating the high purity of the final compounds and efficient elimination of solvents and impurities.

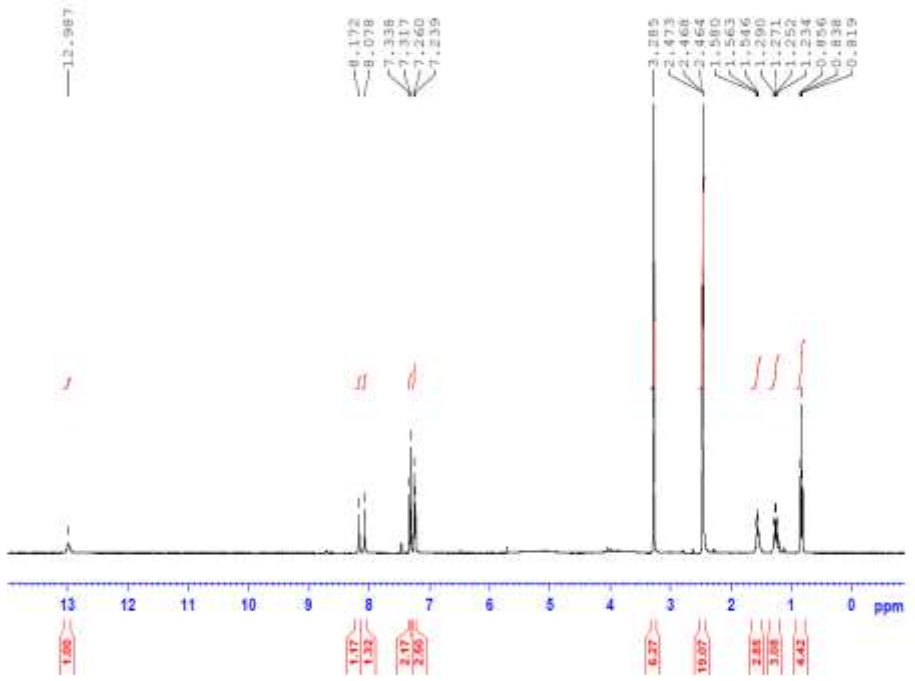

Figure 3: *[1]H-NMR Spectrum of Compound Vt8 in DMSO-d_6 (400 MHz)*

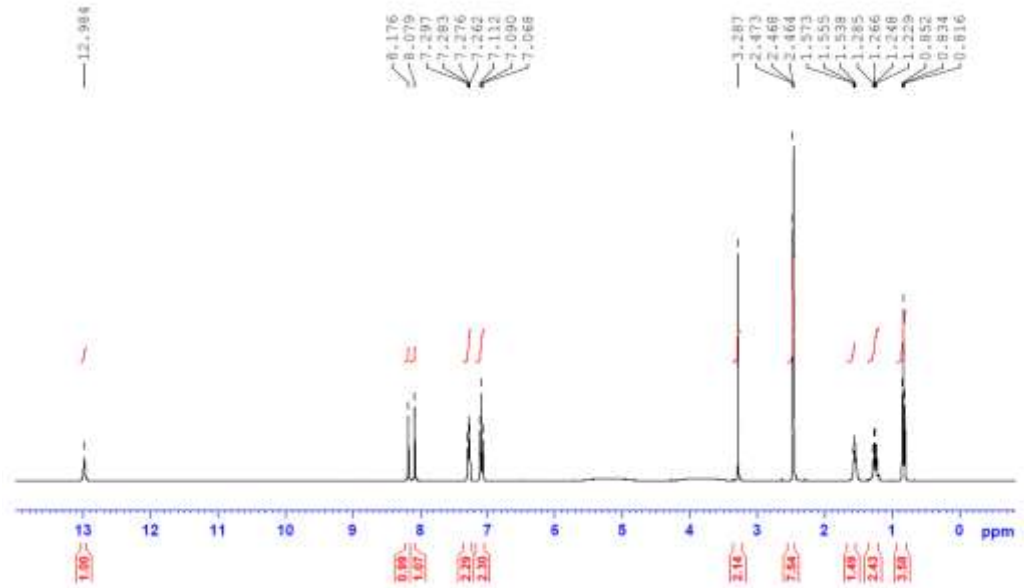

Figure 4: *^{1}H-NMR Spectrum of Compound Vt9 in DMSO-d_6 (400 MHz)*

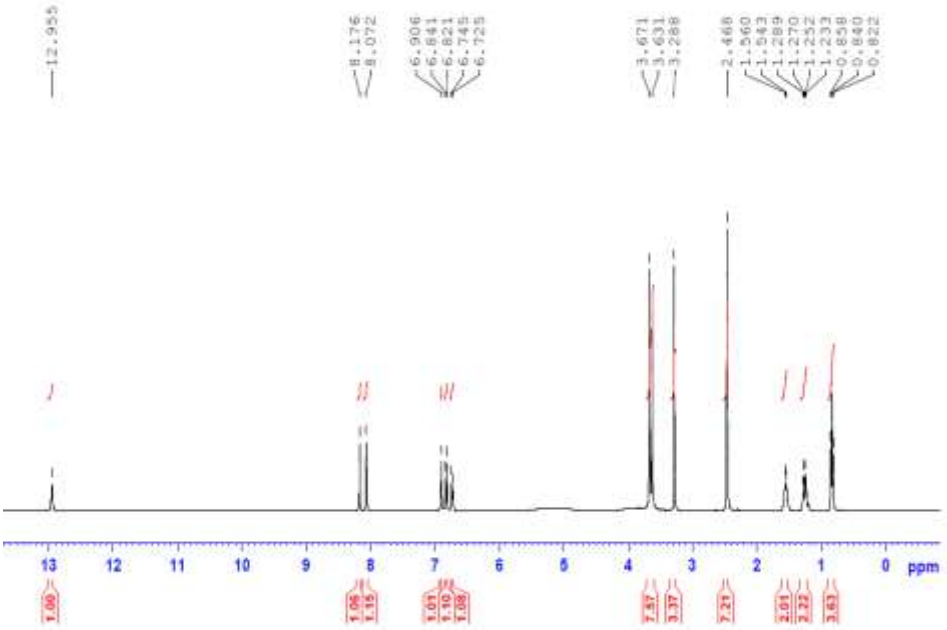

Figure 5: *^{1}H-NMR Spectrum of Compound Vt11 in DMSO-d_6 (400 MHz)*

Table 2: Physicochemical and Spectral Data of Synthesized 1,3,4-Oxadiazole–Linked Benzothiazole Derivatives

Compound Code	Yield (%)	Melting Point (°C)	Rf Value	Mol. Wt. (g/mol)	FTIR (cm^{-1})	^{1}H-NMR (δ ppm)	$[M+H]^+$ (m/z)

Vt8	80%	172–174	0.72	342.08	3305 (N–H), 1654 (C=O), 1588 (C=N)	7.12–8.14 (Ar-H), 10.76 (NH)	343
Vt9	76%	165–167	0.69	356.11	3312, 1660, 1592	7.01–8.08, 10.85	357
Vt10	71%	153–155	0.66	348.09	3290, 1648, 1601	7.08–8.02, 11.00	349
Vt11	78%	175–177	0.70	360.12	3340, 1657, 1585	7.15–8.18, 10.95	361
Vt12	68%	148–150	0.61	338.06	3301, 1638, 1598	7.03–8.10, 11.10	339

3.1.5 Pharmacological Activity

The synthesized benzothiazole–oxadiazole hybrids were screened for anti-inflammatory and central analgesic activities using carrageenan-induced paw edema and Eddy's hot plate methods respectively, in Wistar rats. The results were compared with reference standards diclofenac sodium (10 mg/kg, p.o.) and pentazocine (10 mg/kg, i.p.) for anti-inflammatory and analgesic studies, respectively. In the carrageenan-induced rat paw edema model, all tested compounds exhibited varying degrees of anti-inflammatory activity. Among them, compound Vt8 demonstrated the highest inhibition of paw edema at the 3rd and 4th hour post-carrageenan injection, showing a maximum inhibition of 63.4%, which was comparable to diclofenac sodium (67.8%). Other compounds such as Vt9 and Vt11 showed moderate activity, while Vt12 showed the least inhibition. The anti-inflammatory effect was observed to be time-dependent, with peak inhibition noted at 3 hours, consistent with the second phase of inflammation involving prostaglandin synthesis. This suggests that the compounds possibly act via COX inhibition mechanisms. In the central analgesic activity test, compound Vt11 exhibited the most significant analgesic effect, with a maximum latency time of 13.6 seconds at 90 minutes, which approached the efficacy of the standard drug pentazocine (14.2 seconds). Vt8 and Vt10 also showed a moderate increase in latency period, indicating potential analgesic effects. The increased latency time suggests that these compounds are capable of crossing the blood-brain barrier and exerting central nervous system activity, potentially through modulation of opioid or prostaglandin pathways. The Structure–Activity Relationship (SAR) analysis revealed that electron-withdrawing substituents, such as $-NO_2$ or –Cl, on the phenyl ring attached to the oxadiazole moiety, enhanced anti-inflammatory activity, as observed in Vt8. In contrast, electron-donating groups such as $-OCH_3$ or $-CH_3$ contributed more towards central analgesic effects, as seen with Vt11. This suggests that steric and electronic factors at the periphery of the hybrid scaffold play a crucial role in determining pharmacological selectivity. The observed pharmacological profile indicates that the dual heterocyclic system confers multi-target potential, and with further optimization, these compounds may serve as effective leads for inflammatory and pain-related disorders. The comparative performance of the synthesized molecules relative to standard drugs confirms their therapeutic relevance and supports their advancement into chronic pharmacological models.

Table 3: Anti-inflammatory and Analgesic Activities of Synthesized Compounds

Compound Code	**% Inhibition (at 3h)**	**% Inhibition (at 4h)**	**Latency Time at 90 min (sec)**	**Remarks**
Control (CMC)	0	0	4.2	—
Diclofenac	65.3%	67.8%	—	Standard Anti-inflammatory
Pentazocine	—	—	14.2	Standard Analgesic
Vt8	61.0%	**63.4%**	10.8	**Best anti-inflammatory**
Vt9	49.2%	52.6%	9.6	Moderate activity

Vt10	44.7%	48.3%	10.2	Mild anti-inflammatory, moderate analgesic
Vt11	52.5%	54.1%	**13.6**	**Best analgesic**
Vt12	38.0%	41.2%	8.1	Least effective

3.1.6 Anti-inflammatory Activity (% Edema Inhibition at 3rd Hour)

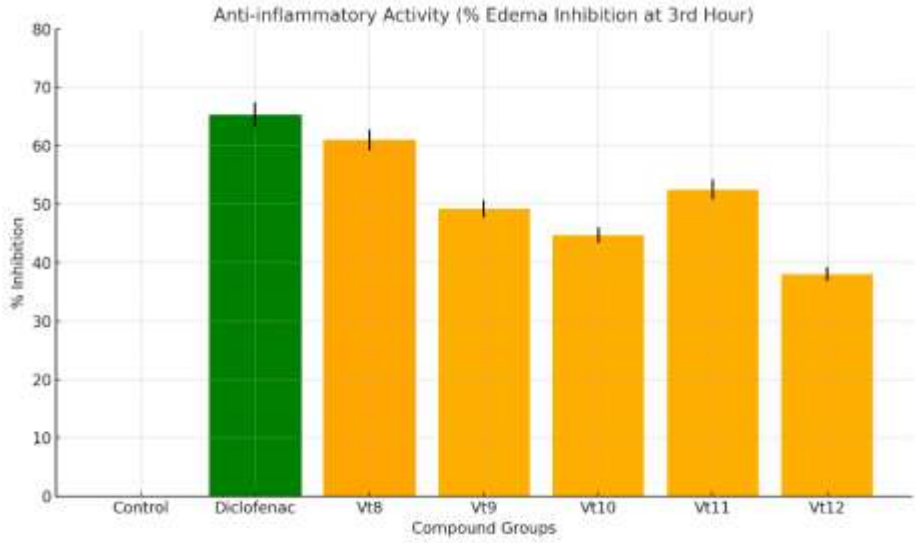

Figure 1: *Comparative anti-inflammatory activity of synthesized benzothiazole–oxadiazole hybrids at 3rd hour post-carrageenan administration in rats.*

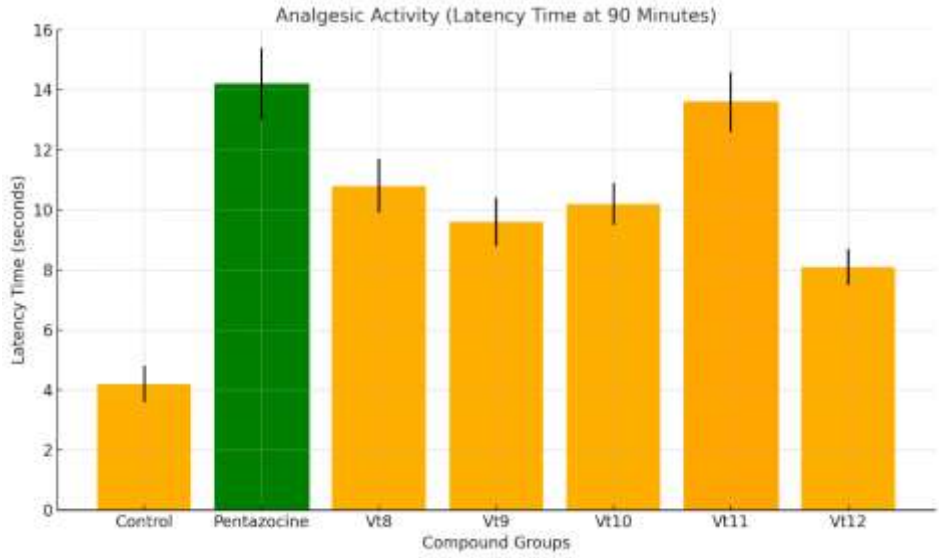

Figure 2: *Evaluation of central analgesic activity of test compounds using Eddy's hot plate method at 90 minutes post-treatment.*

CONCLUSION

In conclusion, the present research successfully demonstrated the rational design and synthesis of novel 1,3,4-oxadiazole-linked benzothiazole hybrids with dual pharmacological actions namely, anti-inflammatory and

central analgesic activities. The synthesized compounds were structurally characterized using FTIR, ^{1}H-NMR, and mass spectrometry, confirming the formation of the desired molecular frameworks. Among the series, compound Vt8 emerged as the most potent anti-inflammatory agent, showing activity comparable to the standard diclofenac, whereas compound Vt11 displayed significant central analgesic activity, nearing the effect of the reference drug pentazocine. The biological evaluations not only validated the therapeutic potential of these hybrids but also highlighted the importance of specific structural features, such as electron-releasing and hydrophobic substituents, in modulating their pharmacological profiles. The integration of benzothiazole and oxadiazole pharmacophores provided a synergistic scaffold that may serve as a valuable lead for the development of multitarget agents in the management of inflammatory pain. These findings open avenues for further optimization and detailed mechanistic studies aimed at developing safe and effective dual-action therapeutics.

REFERENCES:

[1] F. R. Greten and S. I. Grivennikov, "Inflammation and cancer: Triggers, mechanisms and consequences," *Immunity*, vol. 51, no. 1, pp. 27–41, 2019, doi: 10.1016/j.immuni.2019.06.025.

[2] J. Bullock, S. A. A. Rizvi, A. M. Saleh, *et al.*, "Rheumatoid arthritis: A brief overview of the treatment," *Med. Princ. Pract.*, vol. 27, no. 6, pp. 501–507, 2019, doi: 10.1159/000493390.

[3] Munesh Mani, Preeti Shrivastava, Koppula Maheshwari, Anu Sharma, Trishna Mani Nath, Farhad F Mehta, Bishal Sarkar and Prabhakar Vishvakarma* (2025) Physiological and behavioural response of guinea pig (Cavia porcellus) to gastric floating Penicillium griseofulvum: An in vivo study. J. Exp. Zool. India 28, 0000-0000. DOI: https://doi.org/10.51470/ jez.2025.28.2.0000.

[4] Sarvesh Kumar, M. Manoyogambiga, Shalu Attar, Kiranjeet Kaur, Narpat Singh, Shilpy Shakya, Naveen Sharma and Prabhakar Vishvakarma* (2025) Experimental evaluation of hepatorenal and hematopoietic system responses to Solanum xanthocarpum in Rattus norvegicus: A vertebrate organ-level study. J. Exp. Zool. India 28, 0000-0000. DOI: https://doi.org/ 10.51470/jez.2025.28.2.0000.

[5] S. M. Razavi *et al.*, "Licofelone, a potent COX/5-LOX inhibitor and a novel option for treatment of neurological disorders," *Prostaglandins Other Lipid Mediat.*, vol. 157, p. 106587, 2021, doi: 10.1016/j.prostaglandins.2021.106587.

[6] Sambit Kumar Parida, Prabhakar Vishvakarma, Amol Dagdu Landge, Yasmin Khatoon, Naveen Sharma, Subham Kumar Dogra, Farhad F Mehta and Umesh Kumar Sharma (2025) Spatiotemporal biointeraction and morphodynamics of a gastro-retentive Saccharopolyspora-derived macrolide system in the vertebrate gut: A study on absorptive microecology and transit kinetics. J. Exp. Zool. India 28, 0000-0000. DOI: https://doi.org/10.51470/jez.2025.28.2.000.

[7] P. Molina-Sánchez *et al.*, "Defective p27 phosphorylation at serine 10 affects vascular reactivity and increases abdominal aortic aneurysm development via Cox-2 activation," *J. Mol. Cell. Cardiol.*, vol. 116, pp. 5–15, 2018, doi: 10.1016/j.yjmcc.2018.01.010.

[8] Deepti Bhagchandani, Shriyanshi, Fahmeeda Begum, Rangisetti Chandra Sushma, Sazedur Rahman Akanda, Sailesh Narayan, Kumari Sonu and Prabhakar Vishvakarma*, "Exploring the Hepatoprotective Synergy of Humulus Lupulus and Silymarin in Mitigating Liver Damage", Biochem. Cell. Arch. Vol. 25, No. 1, pp. 915-919, 2025, DOI: https://doi.org/10.51470/bca.2025.25.1.915.

[9] L. McEvoy, D. F. Carr, and M. Pirmohamed, "Pharmacogenomics of NSAID-induced upper gastrointestinal toxicity," *Front. Pharmacol.*, vol. 12, p. 684162, 2021, doi: 10.3389/fphar.2021.684162.

[10] F. Celotti and S. Laufer, "Anti-inflammatory drugs: new multitarget compounds to face an old problem. The dual inhibition concept," *Pharmacol. Res.*, vol. 43, no. 5, pp. 429–436, 2001, doi: 10.1006/phrs.2000.0784.

[11] Prabhakar Vishvakarma, Jaspreet Kaur, Gunosindhu Chakraborthy, Dhruv Kishor Vishwakarma, Boi Basanta Kumar Reddy, Pampayya Thanthati, Shaik Aleesha and Yasmin Khatoon, "Nephroprotective potential of Terminalia arjuna against cadmium-induced renal toxicity by in-vitro study", J. Exp. Zool. India 2025, Volume: 28, Issue No: 1(January), Page No: 939, DOI: 10.51470/jez.2025.28.1.939.

[12] S. M. I. Mahboubi Rabbani and A. Zarghi, "Selective COX-II inhibitors as anticancer agents: A patent review (2014–2018)," *Expert Opin. Ther. Pat.*, vol. 29, no. 6, pp. 407–427, 2019, doi: 10.1080/13543776.2019.1623880.

[13] Vishvakarma P. Design and development of montelukast sodium fast dissolving films for better therapeutic efficacy. Journal of the Chilean Chemical Society. 2018 Jun;63(2):3988-93.

[14] H. Ulbrich, B. Fiebich, and G. Dannhardt, "Cyclooxygenase-1/2 (COX-I/COX-II) and 5-lipoxygenase (5-LOX) inhibitors of the 6,7-diaryl-2,3–1H-dihydropyrrolizine type," *Eur. J. Med. Chem.*, vol. 37, no. 12, pp. 953–959, 2002, doi: 10.1016/S0223-5234(02)01418-6.

[15] M. Laube *et al.*, "2,3-Diaryl-substituted indole based COX-II inhibitors as leads for imaging tracer development," *RSC Adv.*, vol. 4, no. 73, pp. 38726–38742, 2014, doi: 10.1039/C4RA05650G.

[16] A. K. Tewari *et al.*, "Synthesis, biological evaluation and molecular modeling study of pyrazole derivatives as selective COX-II inhibitors and anti-inflammatory agents," *Bioorg. Chem.*, vol. 56, pp. 8–15, 2014, doi: 10.1016/j.bioorg.2014.05.004.

[17] B. Hinz and K. Brune, "Cyclooxygenase-II 10 years later," *J. Pharmacol. Exp. Ther.*, vol. 300, no. 2, pp. 367–375, 2002, doi: 10.1124/jpet.300.2.367.
[18] W. Xie *et al.*, "Expression of a mitogen-responsive gene encoding prostaglandin synthase is regulated by mRNA splicing," *Proc. Natl. Acad. Sci. U. S. A.*, vol. 88, no. 7, pp. 2692–2696, 1991, doi: 10.1073/pnas.88.7.2692.
[19] D. Picot, P. J. Loll, and R. M. Garavito, "The X-ray crystal structure of the membrane protein prostaglandin H2 synthase-1," *Nature*, vol. 367, no. 6460, pp. 243–249, 1994, doi: 10.1038/367243a0.
[20] M. Miciaccia *et al.*, "Three-dimensional structure of human cyclooxygenase (hCOX)-I," *Sci. Rep.*, vol. 11, no. 1, p. 4312, 2021, doi: 10.1038/s41598-021-83438-z.
[21] B. J. Orlando and M. G. Malkowski, "Crystal structure of Rofecoxib bound to human cyclooxygenase-II," *Acta Crystallogr. Sect. F Struct. Biol. Commun.*, vol. 72, no. 10, pp. 772–776, 2016, doi: 10.1107/S2053230X16014230.
[22] R. M. Garavito, M. G. Malkowski, and D. L. DeWitt, "The structures of prostaglandin endoperoxide H synthases-1 and -2," *Prostaglandins Other Lipid Mediat.*, vol. 68, pp. 129–152, 2002, doi: 10.1016/S0090-6980(02)00026-6.
[23] L. J. Marnett *et al.*, "Arachidonic acid oxygenation by COX-I and COX-II: Mechanisms of catalysis and inhibition," *J. Biol. Chem.*, vol. 274, no. 33, pp. 22903–22906, 1999, doi: 10.1074/jbc.274.33.22903.
[24] W. L. Smith and R. C. Murphy, *The eicosanoids: cyclooxygenase, lipoxygenase and epoxygenase pathways*, in *Biochemistry of lipids, lipoproteins and membranes*, Elsevier, 2016, pp. 259–296.
[25] M. E. Turini and R. N. DuBois, "Cyclooxygenase-II: A therapeutic target," *Annu. Rev. Med.*, vol. 53, no. 1, pp. 35–57, 2002, doi: 10.1146/annurev.med.53.082901.103952.
[26] A. L. Blobaum and L. J. Marnett, "Structural and functional basis of cyclooxygenase inhibition," *J. Med. Chem.*, vol. 50, no. 7, pp. 1425–1441, 2007, doi: 10.1021/jm0613166.